Electronic Supplementary Material (ESI) for Dalton Transactions.
This journal is © The Royal Society of Chemistry 2020

EXPERIMENTAL SECTION

Materials: Magnesium sulfate, anhydrous (>98.0% (titration)), *n*-butyllithium in hexane (for organic synthesis), and chloroform-d_1 (99.8%) were purchased from Kanto Chemical Co., Inc. Tetrahydrofuran (THF), super dehydrated, with a stabilizer (for organic synthesis), hydrogen peroxide (30%), potassium acetate, europium(III) acetate *n*-hydrate (99.9%), and picene (sublimation) were purchased from Wako Pure Chemical Industries, Ltd. Bromine (>98.0%), palladium(II) acetate (>98.0%), and diphenylphosphine (>90.0%) were purchased from Tokyo Chemical Industry Co., Ltd.

General methods: Electrospray ionization (ESI) mass spectrometry was performed using a JEOL JMS-T100 LP instrument. ^{1}H-NMR spectra were recorded in $CDCl_3$ on a JEOL ECS-400 (400 MHz) spectrometer; $CHCl_3$ (δ_H = 7.26 ppm) was used as the internal reference. Elemental analyses were performed using a MICRO CORDER JM10. Diffuse-reflection spectra were recorded with a JASCO V-670 spectrophotometer equipped with an integrating-sphere unit (JASCO ISN-723). Emission spectra, excitation spectra, and emission lifetimes (λ_{ex} = 356 nm) for $Eu(hfa)_3(PIPO)_2$ were measured using a Horiba FluoroLog®3 spectrofluorometer. Thermogravimetric analyses (TGA) were performed using an EXSTAR 6000 TG/DTA 6300 instrument (Seiko Instruments Inc.). DSC measurements were recorded on a SII DSC 7020 heat flux meter (5 ºC / min). XRD data were recorded at on a Rigaku SmartLab diffractometer with Cu-Kα radiation and D/teX Ultra detector covering 5–35° (2θ).

Preparation of 5-bromopicene:

Picene (1.00 g, 3.59 mmol) was dissolved in chlorobenzene (100 ml). Br_2 (0.19 ml, 3.60 mmol) was added to a solution, and the solution was stirred for 33 h at 60°C. The reactant was cooled to 0 °C. The obtained powder was filtrated. The solid powder is washed with ethanol. Yield: 75% (967 mg, 2.71 mmol)

^{1}H-NMR (400 MHz, $CDCl_3$/TMS) δ/ppm = 9.14 (s, 1H), 9.02-8.91 (m, 2H), 8.86 (t, 2H, *J* = 7.6 Hz, 8.4 Hz), 8.70 (d, 1H, *J* = 9.7 Hz), 8.47 (dd, 1H, *J* = 6.3 Hz, 2.1 Hz), 8.05 (dd, 2H, *J* = 4.4 Hz, 9.2 Hz), 7.82-7.44 (m, 3H), 7.68 (t, 1H, *J* = 8.0 Hz, 8.4 Hz).

Preparation of 5-diphenylphosphorylpicene (PIPO): A solution of potassium acetate (333 mg, 3.40 mmol) and palladium acetate (7.0 mg, 3.00×10^{-2} mmol) were added dropwise to a solution of 5-bromopicene (967 mg, 2.71 mmol) in dry DMA (50 ml).[S1] Diphenylphosphine (0.47 ml, 2.7 mmol) was then added to the solution, which was subsequently stirred for 24 h at 100°C. Then 200 ml of water was added to the solution and the powder obtained was filtrated. The product was extracted using CH_2Cl_2 and washed with distilled water before being dried over anhydrous $MgSO_4$. Following evaporation, the powder was dissolved in $CHCl_3$ (50 ml) and the resulting solution was cooled before the addition of a 30% H_2O_2 aqueous solution (3 ml). The reaction mixture was stirred for 3 h. The product was extracted using $CHCl_3$ and washed with distilled water. The solvent was then evaporated to produce a white powder whose compounds were separated by silica gel chromatography (ethyl acetate: CH_2Cl_2 = 1:4). Recrystallization from CH_2Cl_2/hexane produced transparent crystals. Yield: 38 % (651 mg, 1.36 mmol).

^{1}H-NMR (400 MHz, $CDCl_3$/TMS) δ/ppm = 9.06 (d, 1H, *J* = 9.6 Hz), 8.96 (d, 1H, *J* = 9.2

Hz), 8.90 (d, 1H, *J* = 8.4), 8.84 (d, 1H, *J* = 8.8 Hz), 8.72 (t, 2H, *J* = 8.4 Hz, 9.2 Hz), 8.03 (d, 1H, *J* = 9.2 Hz), 7.96 (d, 1H, *J* = 8.0 Hz), 7.90 (d, 1H, *J* = 9.2 Hz), 7.83 (dd, 4H, *J* = 6.8 Hz, 1.2 Hz), 7.83 (dd, 2H, *J* =6.8 Hz, 5.2 Hz), 7.69-7.62 (m, 3H), 7.59-7.52 (m, 5H); ESI-MS: m/z calcd. for $C_{34}H_{24}OP$, $[M+H]^+$ = 479.16; found: 479.16; elemental analysis calcd. (%) for C 85.34, H 4.84; found: C 84.67, H 4.70.

Preparation of Eu(hfa)$_3$(PIPO)$_2$: Dichloromethane (10 mL) containing Eu(hfa)$_3$(H_2O)$_2$ (406 mg, 0.502 mmol) and PIPO (336 mg, 0.703 mmol) was stirring for 12 h. The reaction mixture was concentrated using a rotary evaporator. Recrystallization from CH_2Cl_2/hexane solution gave transparent crystals Yield: 68 % (409 mg, 0.237 mmol). ESI-MS: m/z calcd. for $C_{78}H_{48}EuF_{12}O_6P_2$, $[M\text{-hfa}]^+$ = 1523.19; found: 1523.18; elemental analysis calcd. (%) for $C_{83}H_{49}EuF_{18}O_8P_2$+0.5$CH_2Cl_2$, C 56.58, H 2.84, found: C 56.99, H: 2.60; IR (ATR) = 1653 (st, C=O), 1252 (st, C-F), 1145 (st, P=O) cm^{-1}.

Calculation of luminescence quantum yields:[S2] The emission quantum yield excited by 4f-4f transition (Φ_{ff}) and the radiative (k_r) and nonradiative (k_{nr}) rate constants were estimated using the following equations:

$$\tau_{rad} = \frac{1}{k_r} \text{(S1)}$$

$$\tau_{obs} = \frac{1}{k_r + k_{nr}} \text{ (S2)}$$

$$\Phi_{ff} = \frac{k_r}{k_r + k_{nr}} = \frac{\tau_{obs}}{\tau_{rad}} \text{ (S3)}$$

$$k_r = A_{MD,0}\, n^3 \left(\frac{I_{tot}}{I_{MD}}\right) \text{ (S4)}$$

$$k_{nr} = \frac{1}{\tau_{obs}} - \frac{1}{\tau_{rad}} \text{(S5)}$$

where n is the refractive index of the medium, $A_{MD,0}$ is the spontaneous luminescence probability for the $^5D_0 \rightarrow {}^7F_1$ transition *in vacuo* (14.65 s^{-1}), and (I_{tot}/I_{MD}) is the ratio of the total area of the Eu(III) luminescence spectrum to the area of the $^5D_0 \rightarrow {}^7F_1$ transition band.

Molecular orbital calculation of PIPO ligands: TD-DFT calculation using the B3LYP functional was performed on simplified models of $Eu(tmh)_3$ using a ligand bonded to a lithium ion to ascertain the electronic structure of the tmh ligand.[S3] TD-DFT calculation was also performed for PIPO to clarify the HOMO level. The calculated HOMO levels of Li-tmh and PIPO are almost same. Thus, PIPO ligand is appropriate for the detection of LMCT effect.

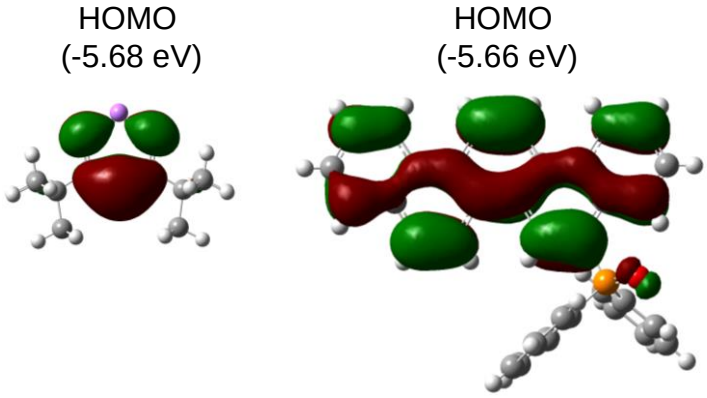

Figure S1 Molecular orbitals of Li-tmh (left) and PIPO (right).

Structure calculation of Eu(III) complex: To obtain an understanding of structure for $Eu(hfa)_3(PIPO)_2$, we calculated the optimized structure between ligands and Eu(III) ions using LUMPAC software.[S4] The ground-state coordination geometries of the Eu(III) complexes was calculated using the Sparkle/RM1 model. The two stable Eu(III) structures were found (Fig. 3, A-form and B-form). The structure of A-form is almost same with the X-ray crystal structure. We used the optimized structures to estimate the singlet and triplet excited states with the configuration interaction singles (CIS) method based on the intermediate neglect of differential overlap/spectroscopic (INDO/S) technique, as proposed in previous reports.[S5-S8] The calculations were performed using ORCA software (v.4.2.0).[S9] We used a point charge (+3) to represent the Eu(III) ion. Estimated singlet (A-form: 29300 cm^{-1}, B-form: 29300 cm^{-1}) and triplet (A-form: 20500 cm^{-1}, B-form: 20300 cm^{-1}) energies of A- and B-form are almost same.

4f-orbital energy calculation: To understand LMCT states of the Eu(III) complexes, DFT calculations [Eu(III): SDD, Other atoms: B3LYP/6-31G(d)] were performed on A- and B-form structures calculated by LUMPAC. The calculated LUMO level of B-form (–2.10 eV) is lower than that of A-form (–1.87 eV). The HOMO-LUMO gap of B-form (3.74 eV) is smaller than that of A-form (3.89 eV).These calculation results indicate that the formation of the LMCT band of B-form in the low energy level originating from the modulation of Eu(III) LUMO levels. This interpretation is consistent with the spectroscopic analysis in the main manuscript.

Single-Crystal X-ray Structure Determination: X-ray crystal structure and crystallographic data for $Eu(hfa)_3(PIPO)_2$ is shown in Fig. 1c, Figure S2, and Table S1, respectively. Measurements were made by using a Rigaku VariMax RAPID imaging-plate diffractometer with confocal mirror-monochromated Mo-Kα radiation. The calculations were performed using Olex2. The CIF data were confirmed by the check CIF/PLATON service. CCDC-1972405) contain the supplementary crystallographic data for this paper. These data can be obtained free of charge from The Cambridge Crystallographic Data Centre via www.ccdc.cam.ac.uk/data_request/cif.

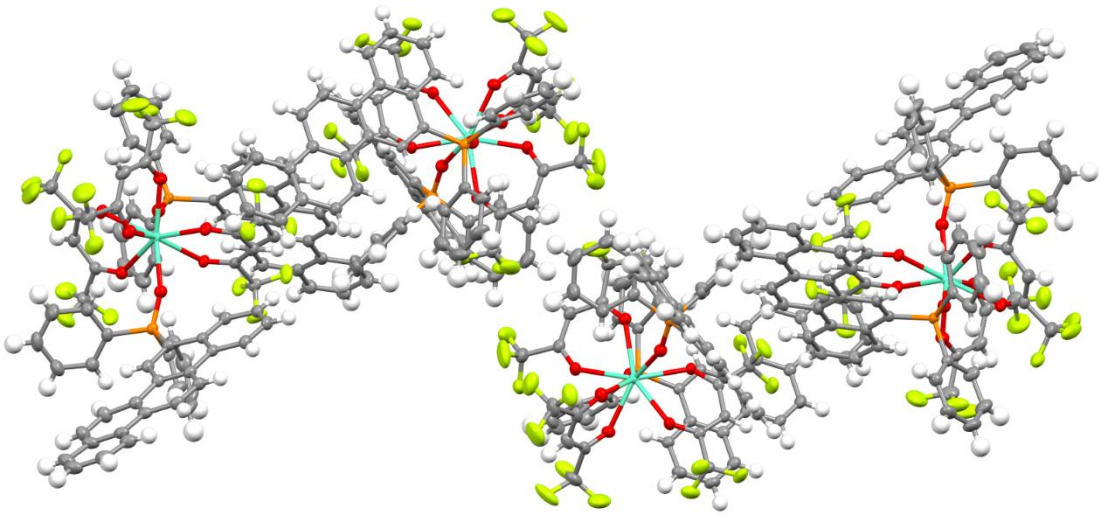

Figure S2 X-ray crystal structure of $Eu(hfa)_3(PIPO)_2$.

Table S1 Single crystal data of $Eu(hfa)_3(PIPO)_2$

	$Eu(hfa)_3(PIPO)_2$
chemical formula	$C_{83}H_{49}EuF_{18}O_8P_2$
formula weight	1730.14
crystal system	monoclinic
space group	P $2_1/n$
a / Å	23.3898(4)
b / Å	14.3443(2)
c / Å	25.8557(4)
α / deg	90
β / deg	107.500(2)
γ / deg	90
volume /Å	8273.4(2)
Z	4
density/g cm^{-1}	1.389
Temperature / ºC	-150
μ (Mo Ka) / mm^{-1}	0.889
max 2θ / deg	57.946
Reflections	116157
Independent refl.	19129
R	0.0541
wR_2	0.1321

Shape measure analysis: The continuous shape measure factor *S* was calculated to estimate the degree of distortion of the coordination structure in the first coordination sphere based on crystal structure data.[S10] The *S* value is given by following equation:

$$S = \min \frac{\sum_k^N |Q_k - P_k|^2}{\sum_k^N |Q_k - Q_o|^2} \times 100 \qquad \text{(S6)},$$

where Q_k denotes the vertices of the actual structure, Q_0 is the center of mass of the actual structure, N is the number of vertices, and P_k denotes the vertices of an ideal structure. From the calculation, $Eu(hfa)_3(PIPO)_2$ was categorized as a TDH (D_{2d}) structure (S = 2.01) with asymmetric coordination geometry.

Emission lifetimes:

We measured emission decays of $Eu(hfa)_3(PIPO)_2$ (A-form, before heating) at ten times using NG-YAG laser (λ_{ex}=355 nm, λ_{em} = 610 nm). The estimated lifetimes are 0.5678, 0. 5681, 0.5702, 0.5650, 0.5672, 0.5681, 0.5680, 0.5708, 0.5697, 0.5707 ms (Average lifetime: 0.5686 ms, deviation: 1.734×10^{-3}, deviation percent: 0.3049 %). Based on the results, we calculated the standard deviation of non-radiative rate constants and emission quantum yields using equations (S1-S5) (Table 1).

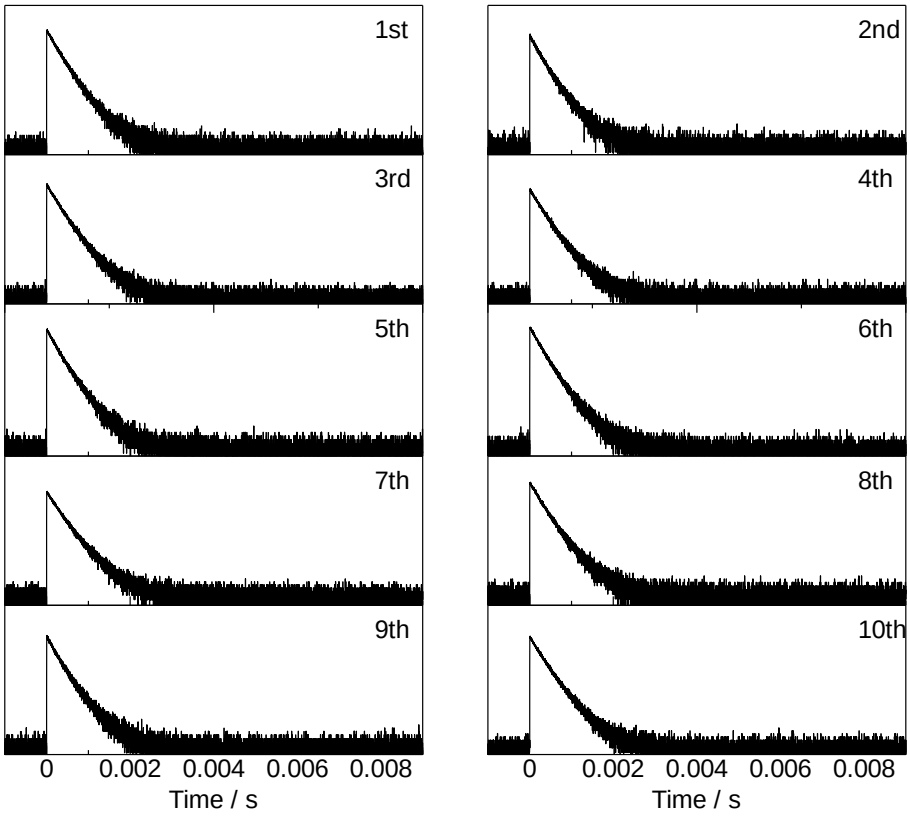

Figure S3. Emission decay curves of $Eu(hfa)_3(PIPO)_2$ (A-form, before heating).

We also measured emission decay of $Eu(hfa)_3(PIPO)_2$ (B-form, after heating) at ten times using NG-YAG laser (λ_{ex}=355 nm, λ_{em} = 610 nm). The estimated lifetimes are 0.6274, 0.6285, 0.6255, 0.6245, 0.6262, 0.6275, 0.6288, 0.6270, 0.6254, 0.6302 ms (Average lifetime: 0.6271 ms, deviation: 1.661×10^{-3}, deviation percent: 0.2649 %). Based on the results, we also calculated the standard deviation of non-radiative rate constant and emission quantum yield using equations (S1-S5) (Table 1).

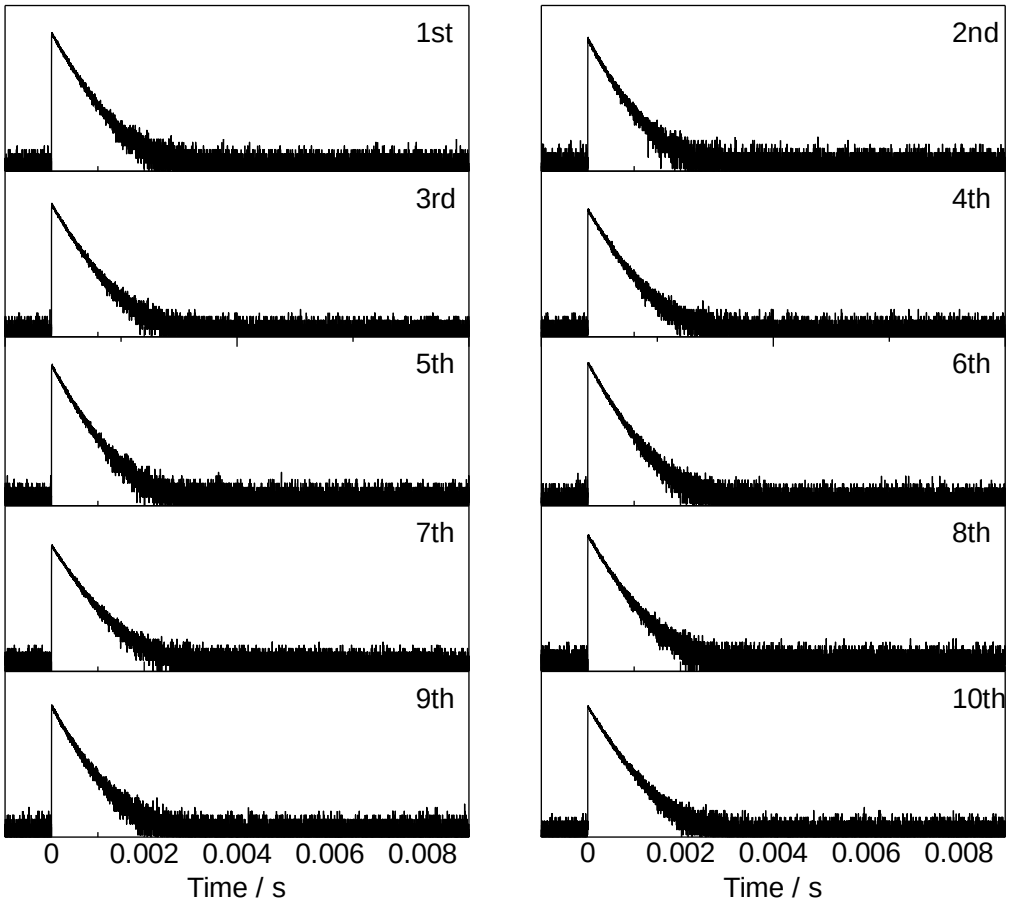

Figure S4. Emission decay curves of $Eu(hfa)_3(PIPO)_2$ (B-form, after heating).

Absorption spectrum:

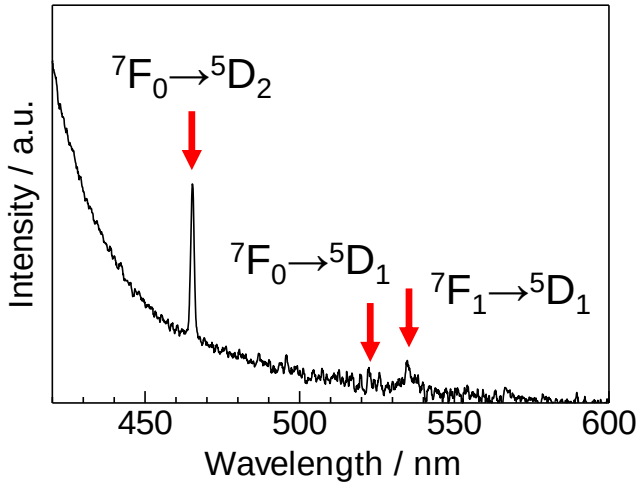

Figure S5. Diffuse reflection spectrum of B-form.

Excitation spectra:

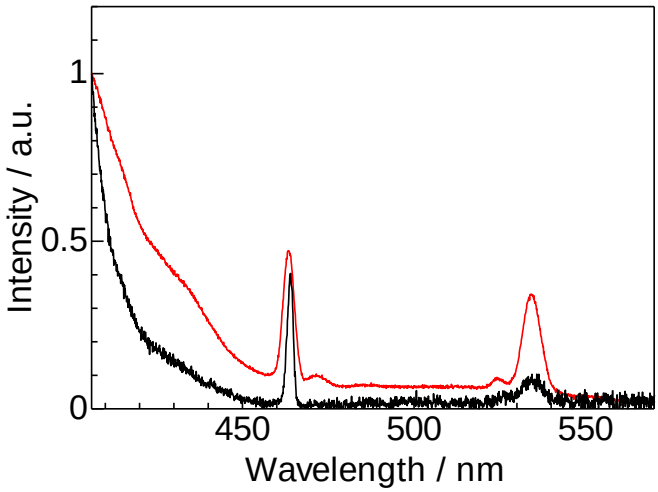

Figure S6. Excitation spectra (λ_{ex} = 610 nm) of A-form (black line) and B-form (red line).

Temperature-dependent emission lifetimes:

To understand change of photophysical properties with phase transition, we also measured emission lifetimes depending of temperature using Fluorolog-3 with cryostat and LED laser (Figure S7). At the phase transition point, the emission lifetime change depending on temperature is changed. The temperature sensitivity in B-form region (0.66 %/K, 450 K-500 K) is relatively similar with that of previous Eu(III) complexes with effective LMCT quenching states.[S11] These results indicated that the phase transition induced changes of LMCT band energy and Eu(III) emission properties.

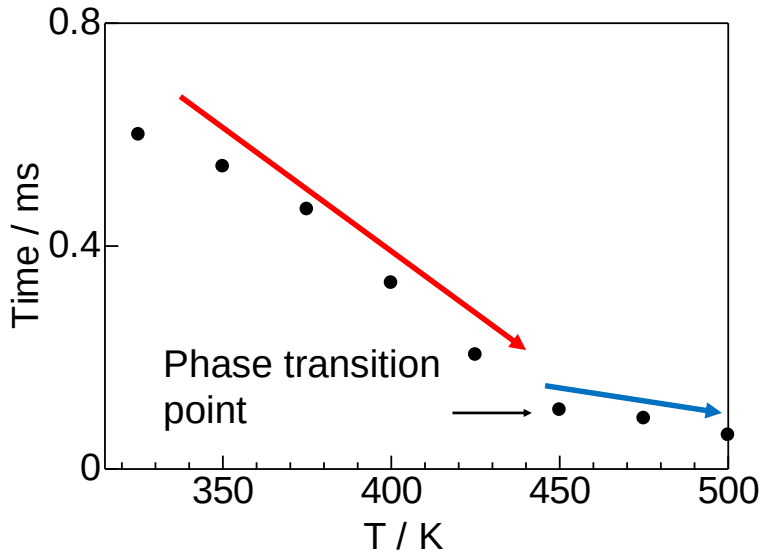

Figure S7. Temperature-dependent emission lifetime (λ_{em} = 610 nm, λ_{ex} = 356 nm). Red and blue arrows indicate the emission lifetime changes in A-form and B-form, respectively.

References

S1. O. Herd, A. Heßler, M. Hingst, M. Tepper and O. Stelzer, *J. Organomet. Chem.* 1996, **522**, 69.

S2. M. H. V. Werts, R. T. F. Jukes and J. W. Verhoven, *Phys. Chem. Chem. Phys.* 2002, **4**, 1542.

S3. S. Omagari, T. Nakanishi, T. Seki, Y. Kitagawa, Y. Takahata, K. Fushimi, H. Ito and Y. Hasegawa, *J. Phys. Chem. A* 2015, **119**, 1943

S4. J. D. Dutra, T. D. Bispo and R. O. Freire, *J. Comput. Chem.* 2014, **35**, 772.

S5. J. E. Ridley and M. C. Zerner, *Theor. Chim. Acta* **1976**, *42*, 223.

S6. J. Andres and A.-S. Chauvin, *Phys. Chem. Chem. Phys.* 2013, **15**, 15981.

S7. J. G. Santos, J. D. L. Dutra, S. A. Junior, R. O. Freire and N. B. da Costa Jr., *J. Phys. Chem. A* 2012, **116**, 4318.

S8. R. Ilmi, A. Haque, M. S. Khan, M. S., *J. Photochem. Photobiol., A: Chem.* 2019, **370**, 135.

S9. F. Neese, *Comput. Mol. Sci.* 2012, **2**, 73.

S10. D. Casanova, M. Llunell, P. Alemany and S. Alvarez, *Chem.–Eur. J.* 2005, **11**, 1479.

S11. K. Yanagisawa, Y. Kitagawa, T. Nakanishi, T. Akama, M. Kobayashi, T. Seki, K. Fushimi, H. Ito, T. Taketsugu and Y. Hasegawa, *Eur. J. Inorg. Chem.* 2017, 3843.